*Proceedings of the*
*Annual Stability Conference*
*Structural Stability Research Council*
*Orlando, Florida, April 12-15, 2016*

# Ultimate Strength of Tapered Bridge Girders Under Combined Bending and Shear

Metwally Abu-Hamd [1], Farah El-Dib [2]

**Abstract**
This paper presents an analytical study of the ultimate strength of tapered plate girders under combined bending and shear. A finite element model subjected to uniform bending stress without shear and to uniform shear stress without bending is developed. Standard imperfection models are applied to the girder model. The model is validated using available test results on web tapered girders. A parametric study is performed to investigate the effect of major design parameters such as web and flange slenderness, tapering angle, tapered panel aspect ratio on the ultimate buckling strength under combined shear and bending loads. The results are then used to develop simplified formulae which represent the interactive relationships of bending and shear for all possible magnitude and direction combinations.

## 1. Introduction

Web tapered girders are usually used in bridges to achieve economy by varying the web depth according to variation of the bending moments and shear forces resulting from applied loads. This variation leads to lighter design than conventional prismatic girders. Current design codes, e.g., AASHTO (2010), are based on theoretical and experimental research on prismatic girders. Theoretical solutions of plate buckling problems are based on the simplifying assumptions of simply supported plate panels. These solutions do not consider the real boundary conditions at the web-flange and web-stiffener connections which are known from experimental investigations to be somewhere between simply supported and fixed depending on the relative slenderness of the flange and the stiffener. Finite Element Analysis has been used effectively to obtain the elastic buckling stress and the ultimate strength under a wide scope of design variables related to applied stresses and actual boundary conditions. Allowance for initial geometric imperfections and residual stresses may be easily incorporated in the finite element model. The buckling stress is obtained by solving a linear eigen-value problem with the eigen-values representing the buckling load factors and the eigen-vectors representing the buckling mode shapes. The ultimate strength is obtained by performing a nonlinear inelastic analysis up to the failure load. The finite element models used may be a single isolated panel or a complete girder model.

[1] Professor, Structural Engineering Dept, Cairo University, Egypt, abuhamd@eng.cu.edu.eg
[2] Lecturer, Housing and Building National Research Center, Egypt.

There are very few theoretical and experimental investigations into the structural behavior of web-tapered girders under shear and/or bending moments, e.g., Mirambell (2000), Real (2010), Studer (2013) and Bedynek (2013). Consequently, there are no specific provisions in current design codes for the design of tapered girders.

## 2- Girder Model

Neither an all edges simply supported plate, nor a single web panel can realistically represent the actual behavior of real plate girders used in practice. The finite element models used may be a single isolated panel or a complete girder model. Numerical solutions obtained from isolated single panel models give conservative buckling strength values as compared to results obtained from complete girder models, e.g., and Abu-Hamd (2011). Therefore, a multi-panel girder model with realistic boundary conditions is used in this study to simulate real girders.

The geometry of the model used in the study is shown in Fig.1, Abu-Hamd (2011), Abu-Hamd et al (2014) and El-Dib (2015. The deeper end web depth $H_1$ is fixed in the numerical study at 2 meters while the smaller end depth $H_2$ is varied between 0.40 meter and 2 meters at 0.40 meter intervals to give different tapering angles $\Phi$ of 0.20 and 0.4. The tapered segment length is varied between 2 and 4 meters at 2 meters intervals to give different tapered panel aspect ratios α of 1, and 2, respectively.

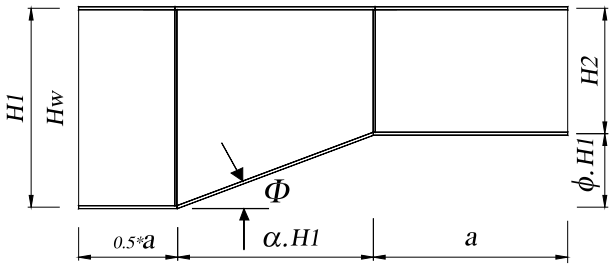


Figure 1: Model geometry

ANSYS (2009) was used to develop the finite element model of the tapered girder. All plate elements were modeled with an iso-parametric finite strain shell element designated as "Shell 181" in ANSYS element library. Shell 181 is a four-node shell element with six degrees of freedom per node and has geometric and material nonlinearities capabilities. It is well suited for linear, large rotation, and /or large strain nonlinear applications. In the construction of the finite element model, convergence was achieved by using a mesh size in the order of 50 mm for all plate elements. The displacement boundary conditions at the left end were specified to give a roller support while the right end was restrained to represent symmetry about the middle vertical plane. Lateral torsional buckling was prevented by restraining the movement in the out-of-plane direction of all nodes along the web-to-flange connection. The material properties used correspond to an elastic-plastic material with Von Mises yield criteria and isotropic hardening. The values of the material constants used are Elastic modulus E=210 GPa, yield stress Fy=350 MPa, and Poisson's ratio ν=0.3.

The loading patterns used are given in Abu-Hamd (2011), Abu-Hamd et al (2014), El-Dib (2015) are distributed around the tapered panel in such a way as to produce pure uniform bending or shear stresses. The model is also subjected to geometrical and structural imperfections as shown in Abu-Hamd (2014).

The interaction between shear and bending loads in maintained for all possible loading combinations by using the following procedure; see Fig. 2 and 3:

The ray *OS* is the start value, usually equals $F_y$, then the iteration proceeds until convergence by keeping the value of the angle $\theta$ unchanged until the destination at point *F*. The ratio of the shear to bending stresses is given by the value of tan $\theta$, noting that the coordinates of *OF* may exceed the ultimate strength under pure bending or pure shear, which explains the necessity of this technique. In Fig. 3 all the categories given in (Bedynek et al 2013) are represented by the types 1 to 4, found by changing the directions of bending and shear forces, which give four different combination possibilities. Type 1 contains positive moment and shear stresses, where positive moment creates compression in the upper flange; and positive shear, acting upwards on the right panel edge creates long tension diagonal (LD). Changing directions and signs of the stresses creates Types 2 to 4. These assignments are respected in all the following ultimate strength figures.

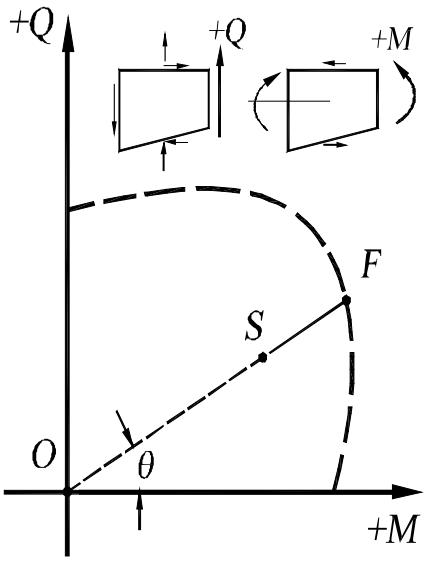


**Figure 2: Radial Evaluation**

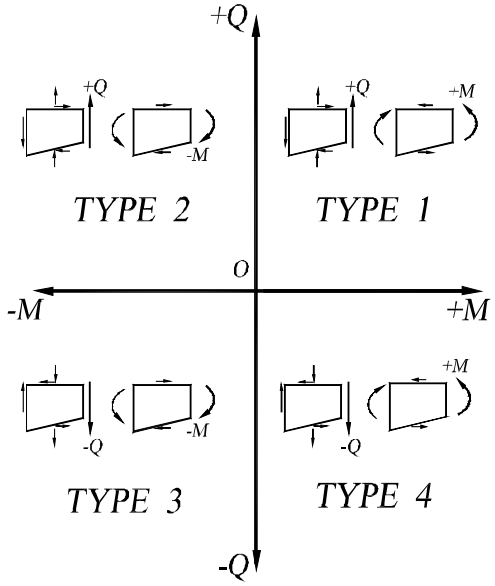


**Figure 3: Loading combinations**

## 2. Ultimate loads under pure stresses

To simplify the representation of the ultimate strength values under combined loading, it is convenient to normalize them with respect to the corresponding values under pure strengths, which are given in Abu-Hamd et al (2014) and El-Dib (2015).

The ultimate shear buckling strength for the tapered girder can be computed from the AASHTO equation for prismatic girders using an equivalent girder depth $H_e$ given by:

For pure shear creating a tension field on the long diagonal "LD"

$$\frac{H_e}{H_w} = \frac{21.\lambda_f^{\,0.1\alpha}.(1+\alpha.\tan^4\Phi)}{\alpha^{0.46}.\lambda_w^{0.7}}. \tag{1}$$

For pure shear creating a tension field on the short diagonal "SD"

$$\frac{H_e}{H_w} = \frac{21.\lambda_f^{\,0.1\alpha}.(1-\alpha.\tan^4\Phi)}{\alpha^{0.46}.\lambda_w^{0.7}}, \tag{2}$$

where $H_e$ is the equivalent depth of a prismatic plate used to get the ultimate shear by applying the well known method AASHTO (2010); $\lambda_f = b / (2*t_f)$ is the flange slenderness; $\alpha$ is the aspect ratio between panel length and maximum depth $H_1$; $\lambda_w = H_w/t_w$ is the web slenderness based on maximum depth $H_w = H_1$ as indicated in Fig. 1; $\Phi$ is the tapering angle of inclination; $t_w$ is the web thickness; $b$ is the flange breadth; and $t_f$ is the flange thickness.

To determine the ultimate load of tapered web girders under uniform bending stresses with a reasonable accuracy, the following approximate equation developed in El-Dib (2015) can be used to represent both cases of Positive and Negative Moment Loading (PL and NL), creating compression in the upper or lower flange respectively:

$$\frac{F_{ult}}{F_y} = (1+0.25\tan\Phi)(1.15-0.02\lambda_f\ -0.001\lambda_w). \tag{3}$$

## 3. Model Validation

The developed finite element model has been validated by comparing its results with some available analytical and experimental results. Fig. 4 shows the comparison with the analytical solution based on Timoshenko (1936) for the case of a rectangular plate with $\lambda_w$ = 100, 140, 200. Fig. 5 shows the comparison with the analytical model developed by Abu-Hamd (2011) for tapered girders with $\lambda_w$ = 100, 140, 200 under pure bending stresses. Table 1 shows a comparison with test results given by Bedynek et al (2013) by assuming small imperfections and

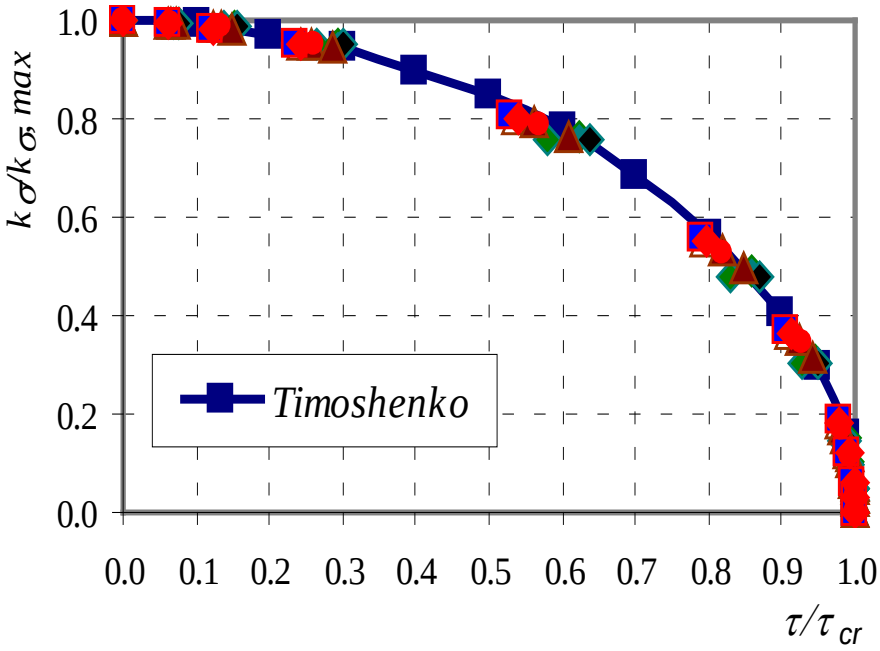


**Fig. 4. Comparison with Timoshenko (1936) for Rectangular Plate with α = 0.667, φ = 0.0 and $\lambda_w$ = 100, 140, 200**

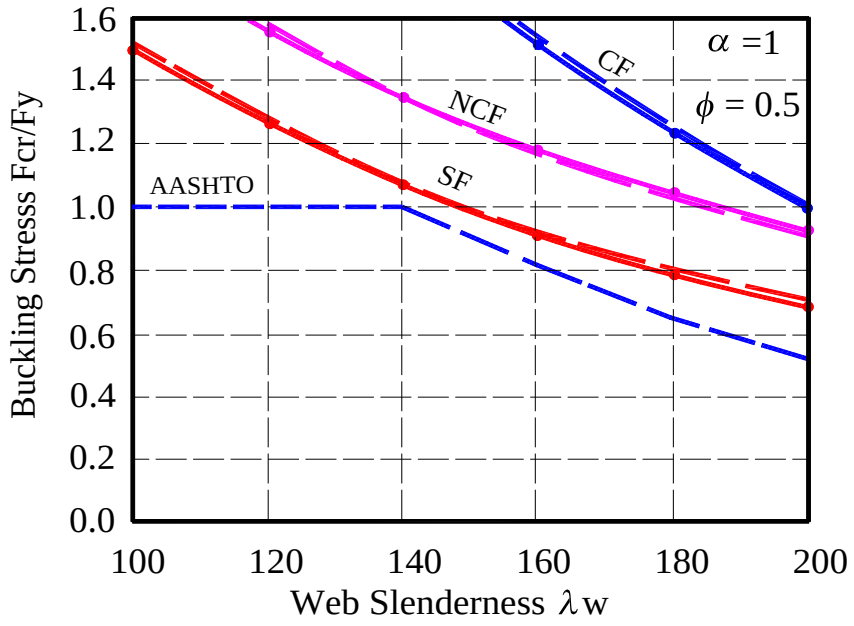


**Fig. 5. Comparison with Abu-Hamd (2011) for Rectangular Plate with α = 1, φ = 0.5 and $\lambda_w$ = 100, 140, 200**

using the present models as shown in Abu-Hamd et al (2014b) and El-Dib (2015). The test specimens were subjected to support shear in addition to bending moments at mid span.

Table 1: Comparison with (Bedynek et al 2013)

| Girder | FEM with Res (Bedynek) | Test Results (Bedynek) | FEM with Res |
|---|---|---|---|
| | $V_u$ (kN) | $V_u$ (kN) | $V_u$ (kN) |
| A 600 800 800 3.9 180 15 | 408.5 | 392.0 | 407.1 |
| B 500 800 1200 3.9 180 15 | 340.6 | 320.5 | 337.7 |
| C 480 800 800 3.9 180 15 | 403.8 | 388.2 | 404.4 |
| D 600 800 800 3.9 180 15 | 421.3 | 425.3 | 420.7 |

The results in Figs. 4 and 5, and all the following plots, are designated according to the following classification:

a) Flange slenderness (CF for compact flange, NCF for non-compact flange and SF for slender flange);
b) Type of failure (C for elastic critical-, RC for relative critical-, U for ultimate load and RU for relative ultimate values);
c) Panel aspect ratio $\alpha$;
d) Tapering (tan $\Phi$); and
e) Web slenderness ($H_w/t_w$),

Note that relative interaction values are normalized w.r.to either to pure bending or to pure shear. The comparison show close agreement between test results and analytical results from the present model.

## 4. Parametric Study

By assuming $\beta = OF/OS$ as the ultimate load multiplier (Fig. 5) the iteration starts usually with $OS = F_y$ and converges at $OF = \beta.F_y$. Thus

$$F_{u,M} / F_y = \beta.\cos\theta, \text{ and} \quad (5)$$

$$Q_{u,Q} / 0.58F_y = \beta.\sin\theta. \quad (6)$$

The evaluation scope includes the following parameters, $\alpha$ = 1.0 to 2.0; tan $\Phi$ = 0.0 to 0.5; flange slenderness from 8 to 18; and web slenderness 100 and 140. Plots of relative ultimate loads are placed close to the plots of ultimate loads for direct comparison. Convergence is achieved by using an element size of 40 – 60 mms.

All plots maintain the arrangement of the loading types as designated in Fig. 3. From Abu-Hamd et al (2014b), selected plots for elastic interaction are demonstrated in Fig. 6. The following plots in Figs. 7 to 10 present the ultimate (U), and the relative ultimate (RU).

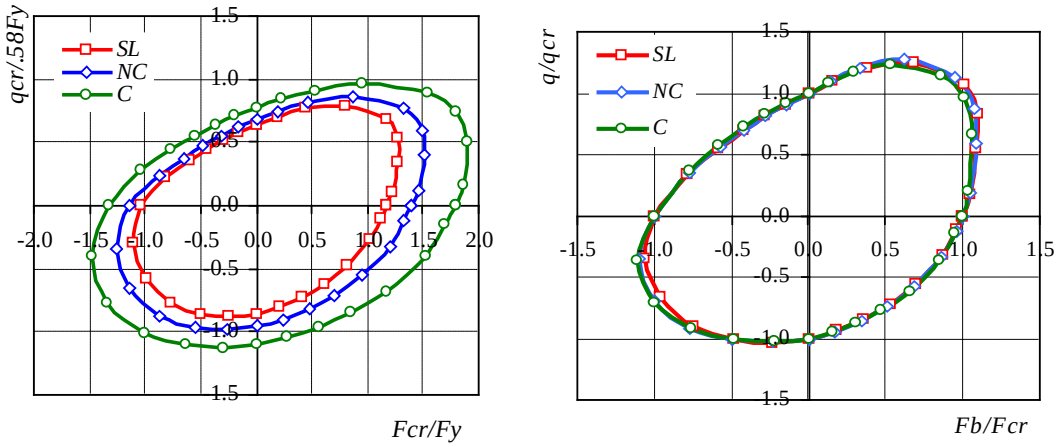


**(a) Critical and Relative Critical Values for $\lambda_w$ = 140**

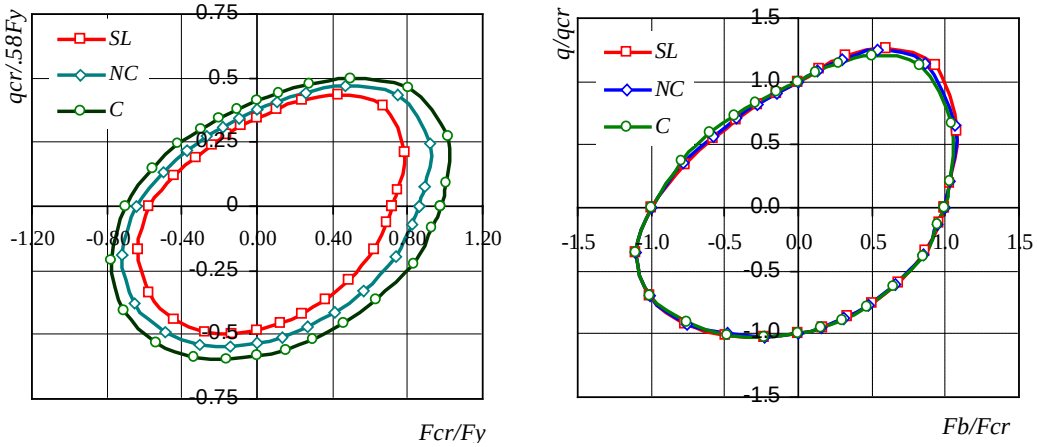


**(b) Critical and Relative Critical Values for $\lambda_w$ = 200**

**Figure 6: Selected Elastic Interaction Diagrams for $\alpha$ = 1.0, tan $\Phi$ = 0.5, Abu-Hamd et al (2014)**

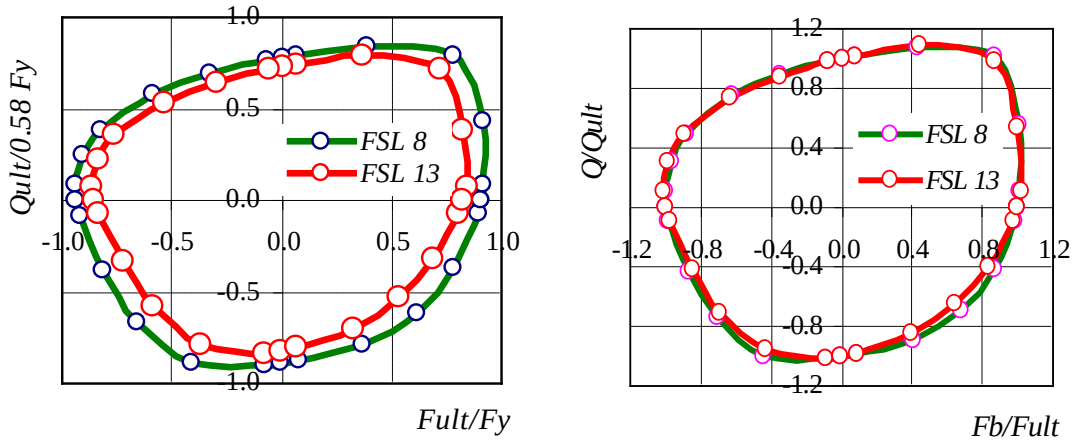


(a) Ultimate and Relative Ultimate Values for tan $\Phi$ = 0.5

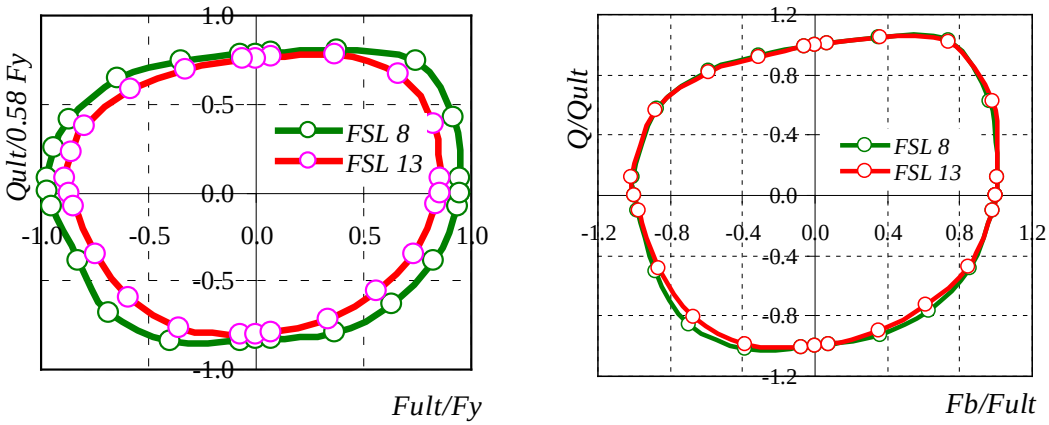


(b) Ultimate and Relative Ultimate Values for tan $\Phi$ = 0.25

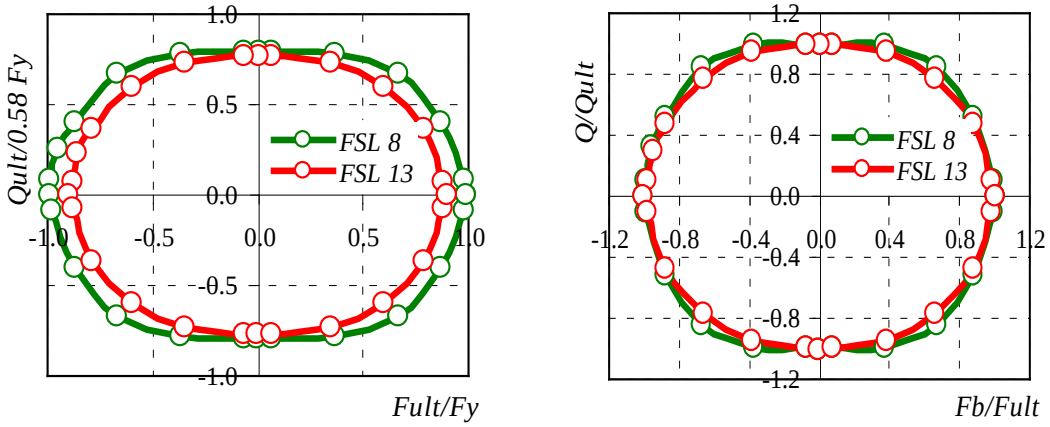


(c) Ultimate and Relative Ultimate Values for tan $\Phi$ = 0

**Figure 7. Ultimate bending and shear interaction ($\alpha$ = 1.0, $\lambda_w$ = 100)**

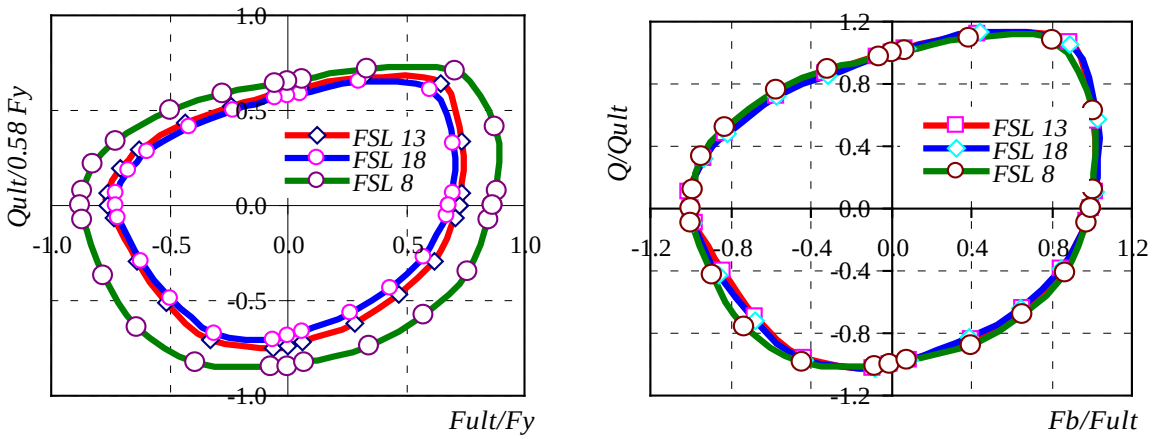


(a) Ultimate and Relative Ultimate Values for tan $\Phi$ = 0.5

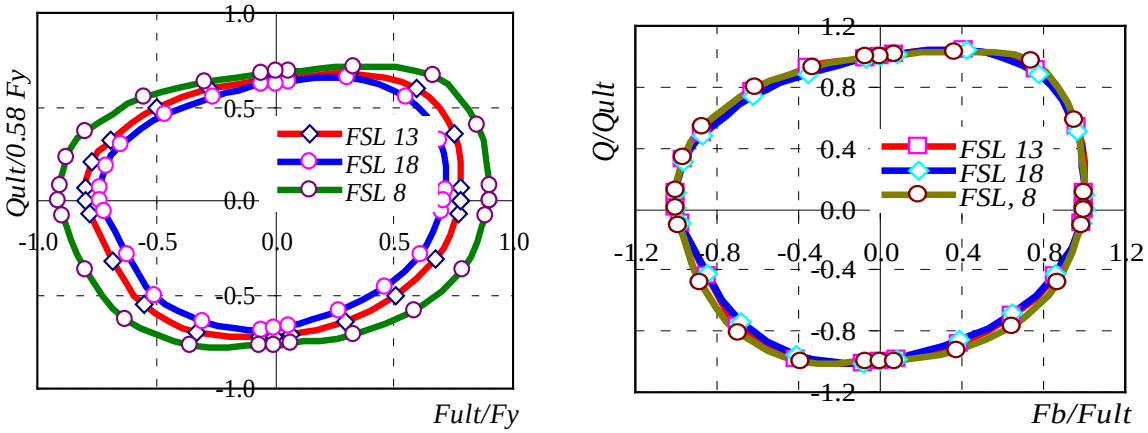


(b) Ultimate and Relative Ultimate Values for tan $\Phi$ = 0.25

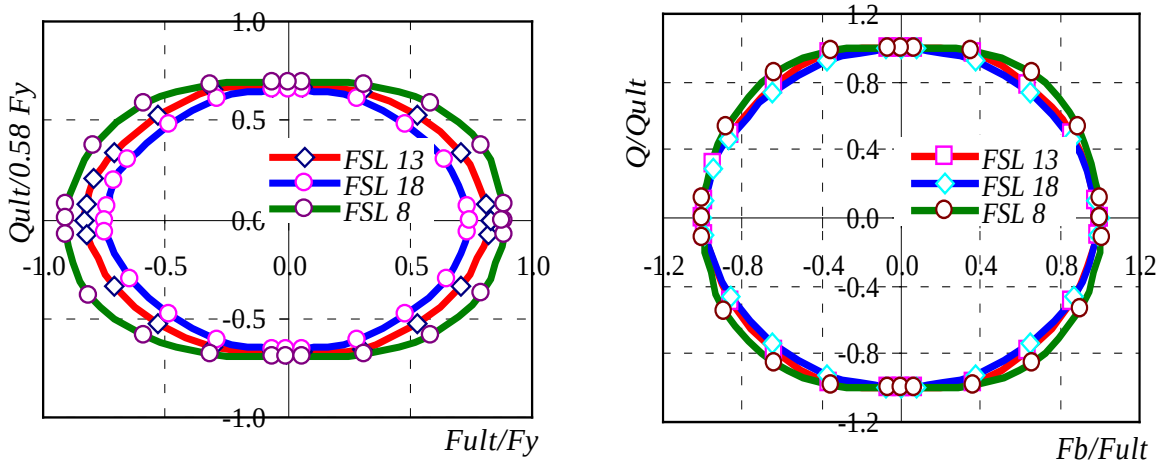


(c) Ultimate and Relative Ultimate Values for tan $\Phi$ = 0

**Figure 8: Ultimate bending and shear interaction ($\alpha$ = 1.0, $\lambda_w$ = 140)**

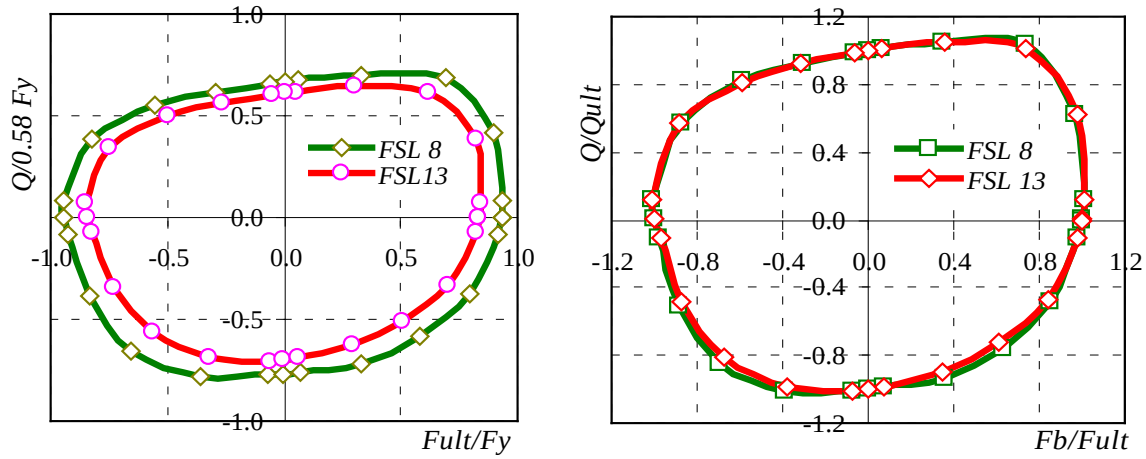


(a) Ultimate and Relative Ultimate Values for tan $\Phi$ = 0.25

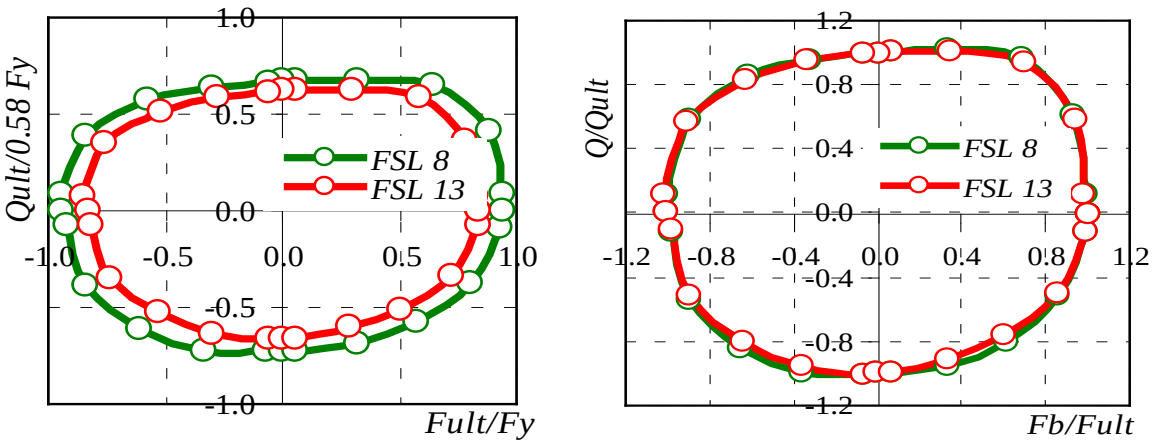


(b) Ultimate and Relative Ultimate Values for tan $\Phi$ = 0.125

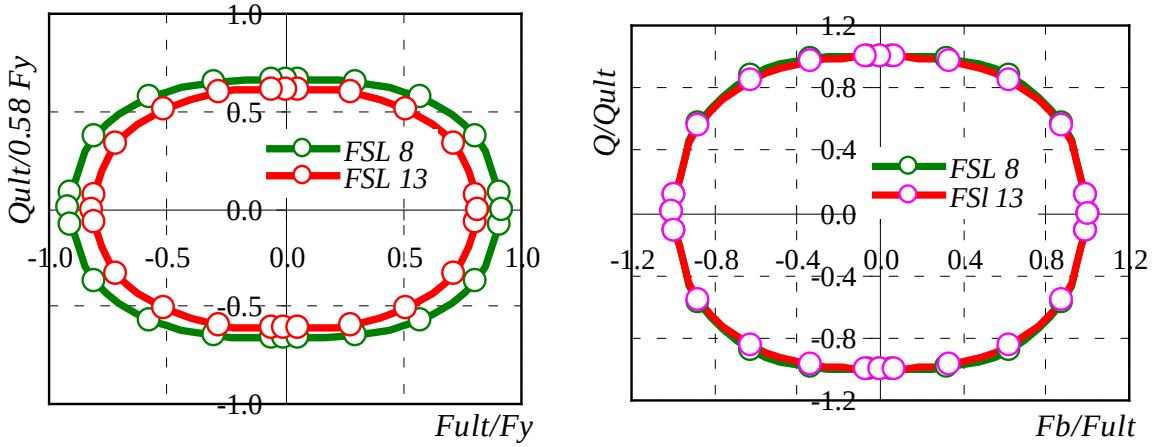


(c) Ultimate and Relative Ultimate Values for tan $\Phi$ = 0

**Figure 9: Ultimate bending and shear interaction ($\alpha$ = 2.0, $\lambda_w$ = 100)**

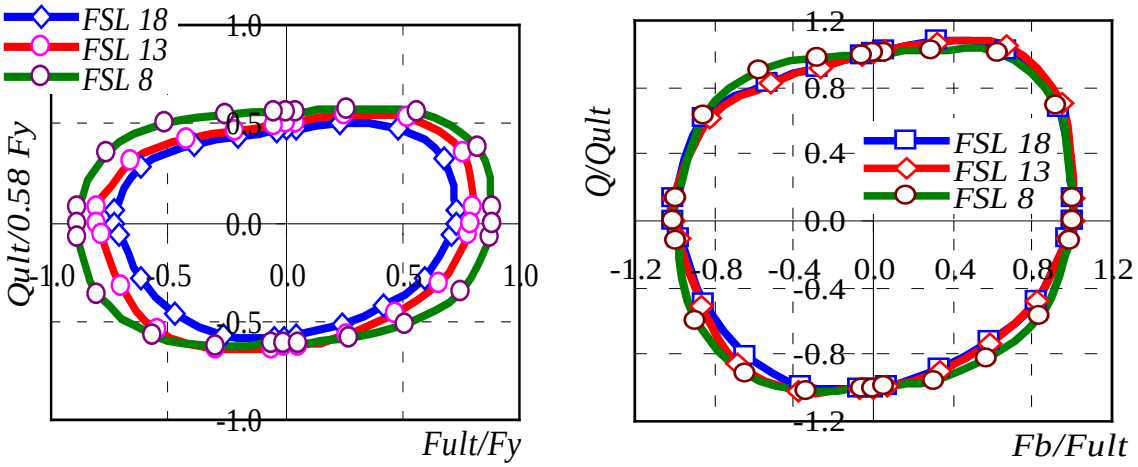


(a) Ultimate and Relative Ultimate Values for tan $\Phi$ = 0.25

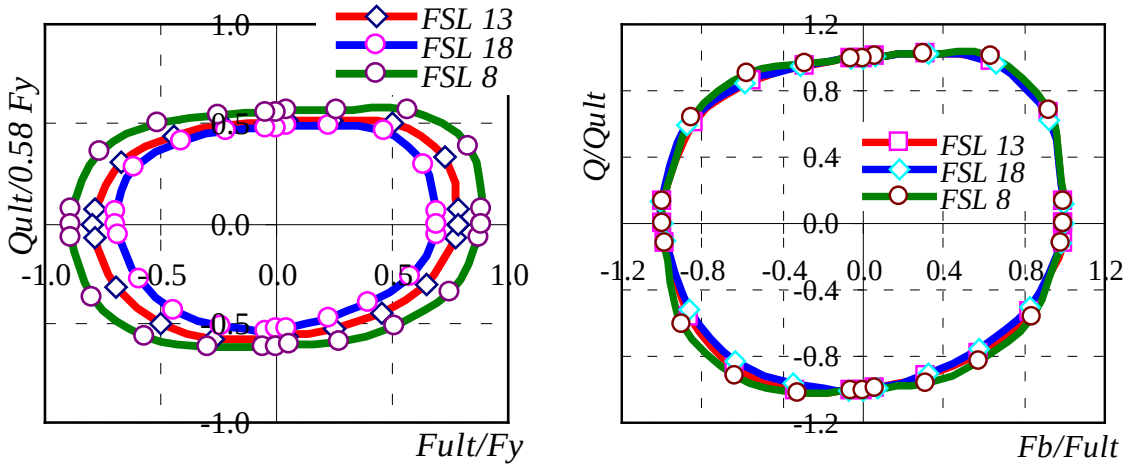


(b) Ultimate and Relative Ultimate Values for tan $\Phi$ = 0.125

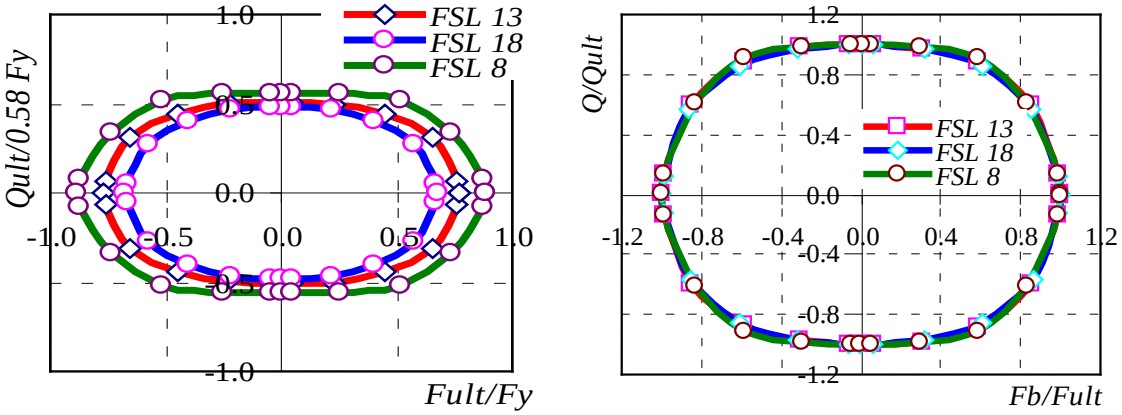


(c) Ultimate and Relative Ultimate Values for tan $\Phi$ = 0.0

**Figure 10: Ultimate bending and shear interaction ($\alpha$ = 2.0, $\lambda_w$ = 140)**

The results of the parametric study are plotted on Fig. 7 to 10. By inspecting the results, we can make the following remarks:

- The flange stiffness remarkably affects the web interaction ultimate resistance, by resisting the web deformations outside its plane.
- A compact flange may increase the interaction ultimate resistance (up to 30%), when bending prevails, but the increase is quite limited in cases with significant shear.
- Increasing the angle of tapering increases in general the ultimate interaction resistance of the tapered web, especially in loading Type 1, where the moment stresses reduce the effect of shear.
- As for $\lambda_w \leq 100$, the failure in this zone is often due to local buckling of the slender flanges that are attached to a stocky web plate.
- The main differences that distinguish ultimate load behavior from elastic buckling are the effect of post buckling and the development of tension fields, the later is noticed even in cases with small amounts of interacting shear stresses.
- When representing the relative interactive results, the plots show that the flange slenderness, as a parameter, almost disappear and becomes irrelevant. We find this phenomenon in elastic buckling, as well as in ultimate loads. Thus, the formulae of the approximate solution do not include the flange slenderness $\lambda_f$.
- The tapering inclination tan $\Phi$ is the major parameter that governs the ultimate load. Those cases with the same tapering inclination, for any aspect ratio $\alpha$, provide almost the same relative interaction relationship.
- To determine the elastic interactive buckling, the bowing of the Eigen-shape, and the elastic stiffness matrix, are found to determine the buckling load. Accordingly the direction of the bending stresses determines whether to reduce the effect of the shear stresses, as found in loading Types 1 and 3, or to increase it, as given in loading Types 2 and 4.
- As for the determination of the ultimate interactive load, the shear stress, once it becomes significant, creates a tension field. This action made the interaction strong as in loading Type 1, but not in case of loading Type 3. Note that Type 3 loading is important for the design of bridge girders with continuous spans.
- The post buckling of the tapered web plate makes the slender plates less sensitive to imperfections, although the selected geometrical imperfection values are conservative.
- The rectangular web plate is implied in the investigation, when the value of tan $\Phi$ is taken as zero.

## 5. Approximate Solution

The following formulae are found adequate to represent the interaction relationships of the ultimate load under combined bending and shear acting on tapered plate girders. The comparative results are found in Figs. 13 to 15. The symbols *T1* to *T4* represent the type of load combination as designated in Fig. 3. Noting that Type 1 is common in simple span girders (Fig. 11) and Type 3 represent the support panel in continuous girders (Fig. 12). Types 2 and 4 are only used in other special cases of loading.

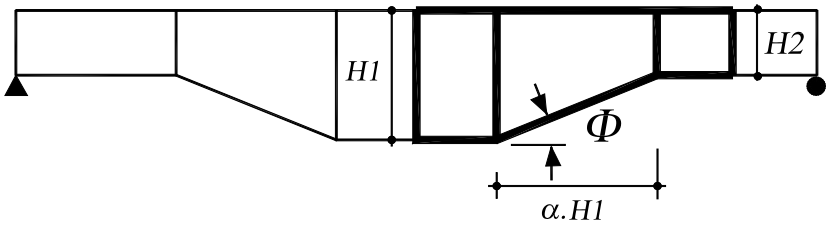


**Figure 11: Example Type 1**

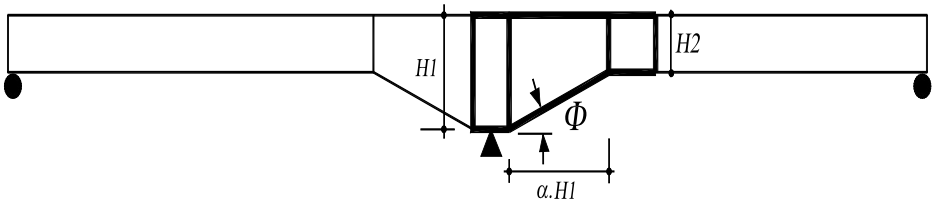


**Figure 12: Example Type 3**

For Type (1),

$$\left(\frac{M_i}{M_{ult}}\right)^A + \left(\frac{Q_i}{Q_{ult}}\right)^A = 1, \tag{7}$$

where $M_i$ and $Q_i$ are the relative interaction bending- and shear stresses; $M_{ult}$ and $Q_{ult}$ are bending and shear ultimate pure stresses as given in Eqs. 1 to 4; and

$$A = 2.0 + 4 \tan \Phi . \tag{8}$$

This type is characterized by increasing the shear resistance due to moment as clearly indicated for loading Type 1 in all plots, noting that no use can be made for $M_i$ or $Q_i$ values above 1.0 for it gives two results and the least one must be taken (*T1* and tan $\Phi$=0.5). For Types (2) and (4)

$$\left(\frac{M_i}{M_{ult}}\right)^B + \left(\frac{Q_i}{Q_{ult}}\right)^B = 1, \tag{9}$$

where $M_i$ and $Q_i$ are the relative interaction bending and shear stresses; $M_{ult}$ and $Q_{ult}$ are bending and shear ultimate pure stresses as given in Equations. 1 to 4; and

$$B = 2.0 - \tan \Phi . \tag{10}$$

Note that these two types show a reduction in the shear resistance due to moments, by increasing the shear effect and are of minor importance in practical design applications. For Type (3)

$$\left(\frac{M_i}{M_{ult}}\right)^C + \left(\frac{Q_i}{Q_{ult}}\right)^C = 1, \tag{11}$$

where, $M_i$ and $Q_i$ are the relative interaction bending- and shear stresses;

$$C = 2.0, \tag{12}$$

$M_{ult} = F_{ult}$, and $Q_{ult}$ are the bending and shear ultimate pure stresses as given in Eqs. 1 to 4.

Comparison with the results of applying these equations are plotted in Figs. 13 to 17.It is clear that the proposed equations can be used to represent the interaction relations between shear and bending for tapered girders.

The results of all investigated cases are reusable, either directly from the respective plot, or by evaluating the simplified empirical formulae. The basic results of loading cases of pure shear and bending stresses are necessary to calculate the relative interaction capacity of tapered web plates. These values are available in Eqs. 1, 2 and 3. It is recommended that design codes consider explicitly the design of the tapered plate girders including their four types of loading.

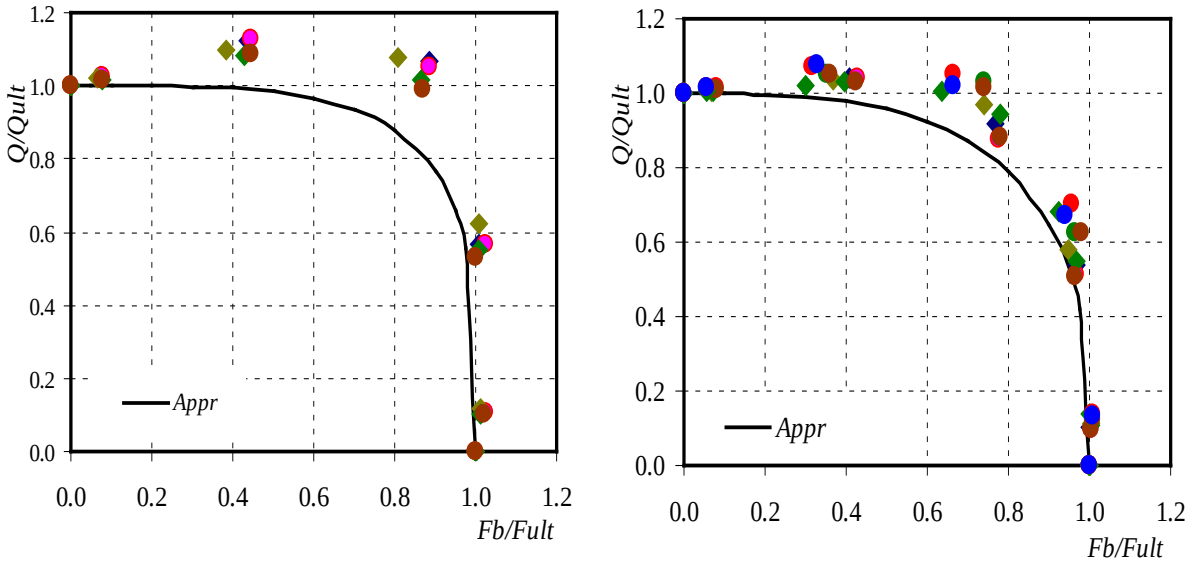


(a) α =1.0, φ = 0.5, $\lambda_w$ = 100,140 (b) α =1,2, φ = 0.25, $\lambda_w$ = 100,140

**Figure 13: Proposed Ultimate Bending and Shear Interaction Formula for Case T1**

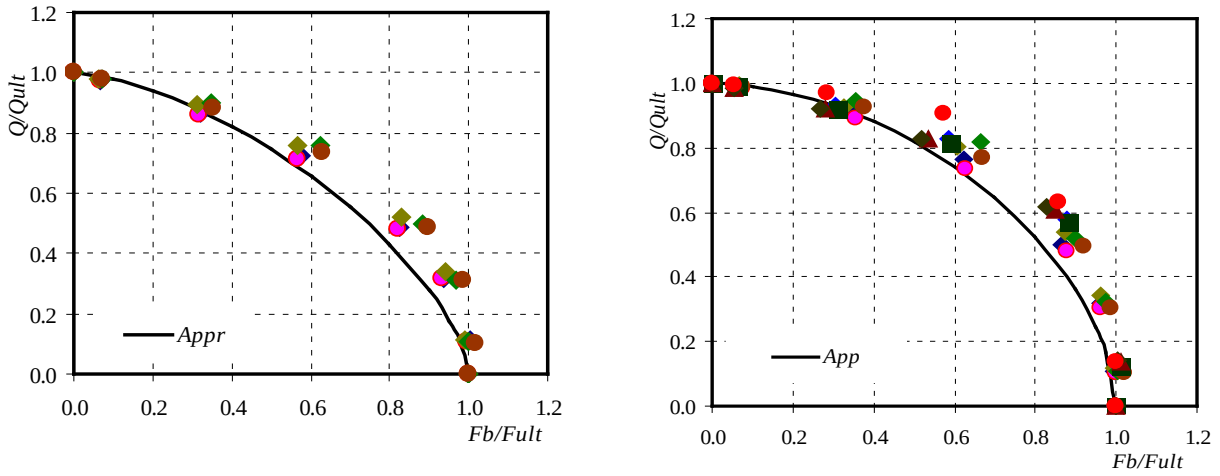


(a) α =1.0, φ = 0.5, $\lambda_w$ = 100,140 (b) α =1,2, φ = 0.25, $\lambda_w$ = 100,140

**Figure 14: Proposed Ultimate Bending and Shear Interaction Formula for Case T2**

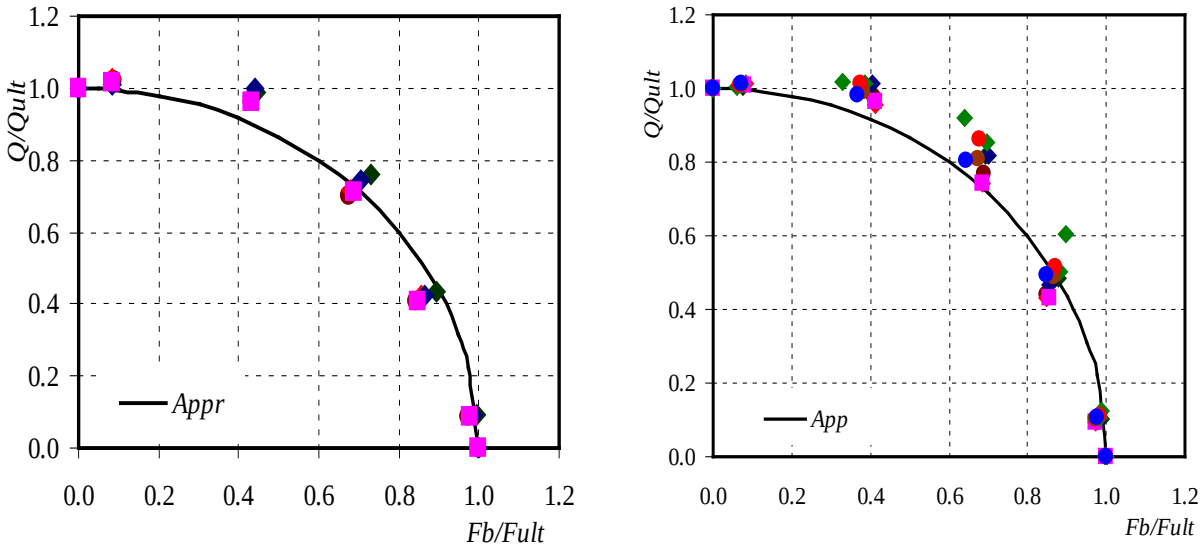


(a) α =1.0, φ = 0.5, $\lambda_w$ = 100,140 (b) α =1,2, φ = 0.25, $\lambda_w$ = 100, 140

**Figure 15: Proposed Ultimate Bending and Shear Interaction Formula for Case T3**

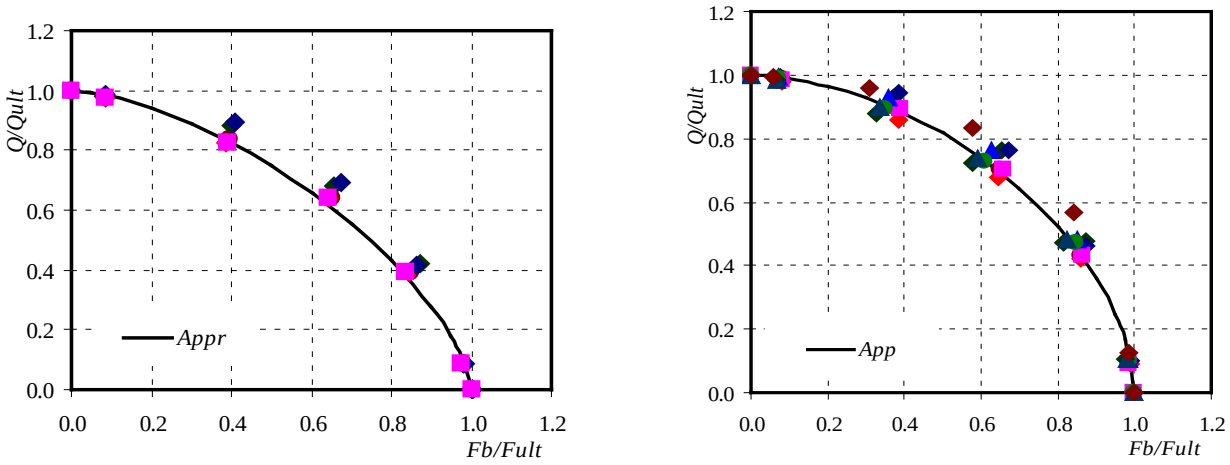


(a) α =1.0, φ = 0.5, $\lambda_w$ = 100,140 (b) α =1,2, φ = 0.25, $\lambda_w$ = 100,140

**Figure 16: Proposed Ultimate Bending and Shear Interaction Formula for Case T4**

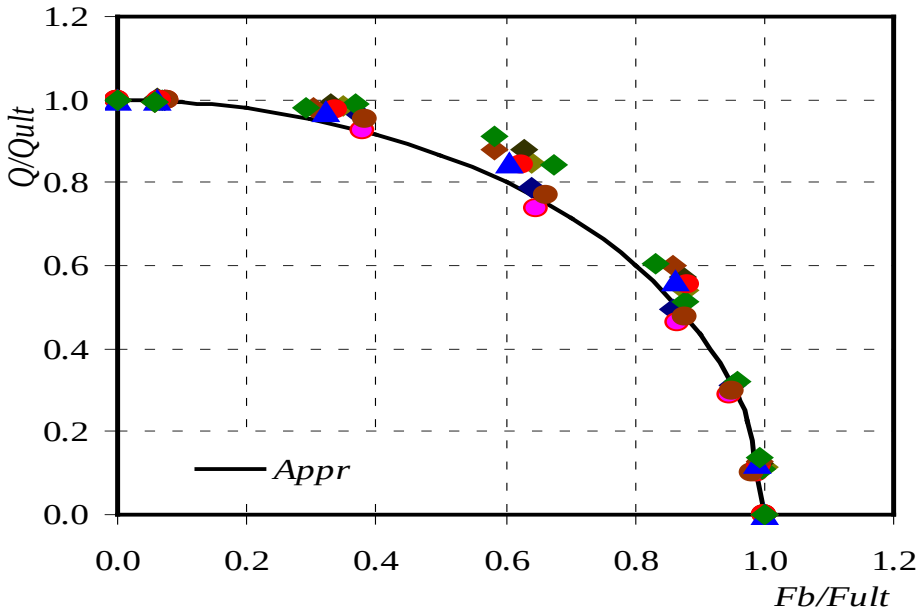


**Figure 17: Proposed Ultimate Bending and Shear Interaction Formula for Prismatic Girders for α =1,2, $\lambda_w$ = 100,140**

## 6. Conclusion

The current investigation determine the ultimate load of a tapered web plate girder under the combination of pure bending and shear stresses, calculated using finite elements. Geometrical imperfections and residual stresses are included in the analysis. It is necessary to calculate first the elastic buckling and use its mode shape to include the geometrical imperfections. The rectangular web plate is within the scope of the present analysis, because it is represented by the special case "tan $\Phi = 0$".

We can numerically investigate and analyze the following problems:

- The elastic stability of a tapered web plate girder under pure shear stresses.
- The ultimate loading capacity, considering structural imperfections of a tapered web plate girder under pure shear stresses.
- The elastic stability of a tapered web plate girder under pure bending stresses.
- The ultimate loading capacity, structural imperfections of tapered web plate girder under pure bending stresses.
- The elastic stability of a tapered web plate girder under combined bending and shear stresses.
- The ultimate loading capacity, considering structural imperfections of a tapered web plate girder under combined bending and shear stresses.

A simplified analytical procedure is given, in form of empirical formulae, along with detailed plots, to reuse the results of each of the above mentioned and studied items.

## References


AASHTO (2009): LRFD Bridge Design Specifications, Washington, D.C.

Abu-Hamd (2010), "Effect of Local Buckling on the Design of Steel Plate Girders", *Proceedings of the Structural Stability Research Council, Annual Stability Conference,* pp 63-82.

Abu-Hamd, et. Al. (2011) "*Buckling* Strength of Tapered Bridge Girders under Shear and Bending*" Proceedings of the Structural Stability Research Council, Annual Stability Conference*.

Abu-Hamd, M., El_Dib (2014b), F. Ultimate Strength of Tapered Web Plate Girder Panels Under Pure Shear, JEAS, Journal of Engineering and Applied Science, (61): 163-82, under publication.

Abu-Hamd, M., El_Dib, F. (2014b) "Buckling Strength of Tapered Bridge Girders under Combined Shear and Bending", HBRCJ, doi:10.1016/j.hbrcj.2014.11.001

AISC. (2010). *Specification for Structural Steel in Buildings,* 14th ed., American Institute of Steel Construction, New York, N.Y.

ANSYS (2009), Theory Manual, Swansea Company.

Barth K. and White D. (1998) "Finite element evaluation of pier moment-rotation characteristics in continuous-span steel I-girders*". Eng Structures,* 20(8):761–78.

Basler, K. (1961). "Strength of plate girders in shear." *J. Struct. Div.*, ASCE, 87(7), 151-180.

Bedynek, A., et. al. (2013), ″Tapered plate girders under shear: Tests and numerical research″ *Engineering Structures*, Issue 46, 350–358.
Earls, C. J. (2007) "Observation on Eigenvalue buckling analysis within a finite element context." *Proceedings of the Structural Stability research Council, Annual Stability Conference.*
El-Dib, F. F. (2015) “Ultimate Strength of Tapered Web Plate Girder Panels Under Combined Bending and Shear”, Ph.D. Thesis, Cairo University, Giza, Egypt,
Maiorana, E., et. al. (2009). “Imperfections in steel girder webs with and without perforations under patch loading.” *Journal of Constructional Steel Research*, Vol 65, pp 1121-1129.
Mirambell, E., et. al. (2000). “Web buckling of tapered plate girders." *Proceedings Inst Civil Eng Struct* , Vol 140, pp 51-60.
Real, E., et. al. (2010). “Numerical and experimental research in tapered steel plate girders subjected to shear .” *SDSS’Rio 2010 Stability and Ductility of Steel Structures*, Batista, E., et al (Eds), pp 747-754.
Timoshenko, S. , (1936). Theory of Elastic Stability”, McGraw-Hill Book Company, p. 355-363
White, D.W. and Barker, M. G., (2008). "Shear Resistance of Transversely Stiffened I-Girders", *ASCE, Jl. Structural Eng.*, 134 (9), 1425-1436.